Domain analysis of cortexillin I: actin-bundling, PIP$_2$-binding and the rescue of cytokinesis

Alexander Stock, Michel O.Steinmetz[1], Paul A.Janmey[2], Ueli Aebi[1], Günther Gerisch[3], Richard A.Kammerer[1], Igor Weber and Jan Faix

Max-Planck-Institut für Biochemie, Am Klopferspitz 18a, D-82152 Martinsried, Germany, [1]Biozentrum der Universität Basel, Klingelbergstrasse 70, CH-4161 Basel, Switzerland and [2]Brigham & Women's Hospital, Harvard Medical School, 221 Longwood Avenue, Boston, MA, USA

[3]Corresponding author
e-mail: gerisch@biochem.mpg.de

Cortexillins are actin-bundling proteins that form a parallel two-stranded coiled-coil rod. Actin-binding domains of the α-actinin/spectrin type are located N-terminal to the rod and unique sequence elements are found in the C-terminal region. Domain analysis *in vitro* revealed that the N-terminal domains are not responsible for the strong actin-filament bundling activity of cortexillin I. The strongest activity resides in the C-terminal region. Phosphatidylinositol 4,5-bisphosphate (PIP$_2$) suppresses this bundling activity by binding to a C-terminal nonapeptide sequence. These data define a new PIP$_2$-regulated actin-bundling site. *In vivo* the PIP$_2$-binding motif enhances localization of a C-terminal cortexillin I fragment to the cell cortex and improves the rescue of cytokinesis. This motif is not required, however, for translocation to the cleavage furrow. A model is presented proposing that cortexillin translocation is based on a mitotic cycle of polar actin polymerization and midzone depolymerization.

Keywords: actin-based membrane flow/cortexillin/green fluorescent protein/mitotic cleavage/phosphatidylinositol 4,5-bisphosphate

Introduction

Cortexillins have been discovered in *Dictyostelium discoideum* as actin-bundling proteins that play a role in cytokinesis (Faix *et al.*, 1996). During mitotic cell division, cortexillins are translocated to the equatorial region of a cell, where they participate in the formation of the cleavage furrow (Weber *et al.*, 1999). Knock-out mutants lacking both cortexillins I and II are dramatically impaired in cytokinesis. These mutants form large, multinucleate cells (Faix *et al.*, 1996). In mutants lacking only cortexillin I the defect in cytokinesis is less severe, but still significant as quantified by counting the number of nuclei per cell (Weber *et al.*, 1999). This defect is paralleled by a reduction in the bending stiffness of the cells, indicating that cortexillins strongly contribute to the mechanical properties of the cell cortex (Simson *et al.*, 1998). *In vitro*

cortexillin I binding to actin filaments is saturable at a ratio of one cortexillin I molecule to three subunits of actin (Faix *et al.*, 1996).

The polypeptide chains of both isoforms, cortexillins I and II, can be subdivided into three distinct domains. An N-terminal domain comprising 226 amino acid residues harbors an α-actinin/spectrin type of actin-binding site. The crystal structure of this type of domain has been determined in fimbrin (Goldsmith *et al.*, 1997). The central region consisting of 18 contiguous heptad repeats dimerizes to form a parallel two-stranded coiled coil (Burkhard *et al.*, 1998; Steinmetz *et al.*, 1998). The C-terminal domain of cortexillin I comprising 92 amino acid residues includes a basic stretch of nine residues at its end, which is reminiscent of a phosphatidylinositol 4,5-bisphosphate (PIP$_2$) binding motif found in other actin regulatory proteins (Janmey *et al.*, 1992).

Studies *in vivo* revealed a crucial role of the C-terminal domain of cortexillin I in translocation of the protein to the cleavage furrow and in the maintenance of cytokinesis (Weber *et al.*, 1999). Here we show that this domain is important for the strong actin-bundling activity of cortexillin I, and that this activity is negatively regulated by PIP$_2$. These data define a new type of actin-binding region of great biological significance.

Results

Cortexillin I lacking the C-terminal domain binds to actin filaments with strongly reduced bundling activity

To determine the role of the N- and C-terminal domains in cortexillin I homodimers, truncated versions of the protein, consisting of the central coiled-coil domain responsible for dimerization and either one of the flanking domains, were purified from lysates of transfected *Escherichia coli* cells. Binding to and bundling of actin filaments were distinguished by high- and low-speed centrifugation. At high speed, corresponding to 100 000 *g*, single actin filaments were pelleted, and cortexillin I constructs co-sedimented with the filaments depending on their binding activity. At low speed, i.e. 15 000 *g*, only bundled or cross-linked actin filaments were pelleted, together with the cortexillin I molecules that cross-linked these filaments. The arrays of actin filaments formed by the cross-linking activities of various cortexillin I constructs were viewed by electron microscopy of negatively stained specimens.

As reported previously (Faix *et al.*, 1996), full-length cortexillin I, comprising 444 residues in each of its two polypeptide chains, caused actin filaments to pellet at low speed and to associate into thick, tight bundles (Figure 1A and B). In principle, a cortexillin I dimer can associate with two actin filaments by virtue of its N-terminal actin-

binding sites, one in each subunit. To determine whether these domains are responsible and sufficient for actin-filament bundling, the C-terminal tail of cortexillin I was removed, leaving the dimerization domain intact. The construct comprising amino acids 1–352 of cortexillin I [designated as CI(1–352)] still bound to actin, but the bundling activity was strongly reduced: only a small fraction of F-actin co-sedimented with CI(1–352) at low

speed. Electron micrographs showed that actin filaments assembled only into loose, indistinct bundles or remained single (Figure 1C).

The binding of CI(1–352) to actin was enhanced at pH 7.0 by a His-tag at its N-terminus, indicating an electrostatic interaction of the positively charged residues of the tag with the negatively charged actin. This interaction was superimposed onto the inherent actin-binding activity of the N-terminal domains. Even using the His-tagged construct, little bundling activity of the C-terminally truncated cortexillin I fragment was disclosed (Figure 1D). We took advantage of the His-tag enhanced decoration of actin filaments in order to visualize the bound cortexillin I fragments by electron microscopy. The N-terminal domains of the fragments associated with single actin filaments so that the 19-nm-long coiled-coil rods were sticking out more or less perpendicular to the filament axis (arrowheads in Figure 1D).

His-tagged or untagged actin-binding domains lacking the dimerization domain [fragment CI(1–233)] bound to actin filaments too weakly to be detectable (data not shown). This finding indicates a cooperation of the two identical N-terminal domains of each dimer in the binding to actin filaments. In order to exert this effect without substantial bundling, the two N-terminal domains of the dimer must bind to actin subunits residing in one and the same filament.

Actin-bundling sites residing in the C-terminal domain of cortexillin I

The weak bundling activity of tailless cortexillin I suggested a second type of actin-binding site residing in the C-terminal region of the cortexillin I molecule. In fact, a headless cortexillin I fragment called CI(227–444) exhibited significant actin-cross-linking activity, although less actin was pelleted than with full-length cortexillin I (compare low-speed centrifugation in Figure 1B with Figure 2A). Electron microscopy revealed thick bundles formed with the headless cortexillin I, together with many actin filaments that remained single. These results indicate that the N-terminal actin-binding domains missing in the CI(227–444) fragment enhance the cross-linking of actin filaments, but they are not essential for bundling.

A distinct sequence element in the C-terminal region of cortexillin I is the lysine-rich stretch of amino acids 436–444 at the very end of the polypeptide chain. Elimination
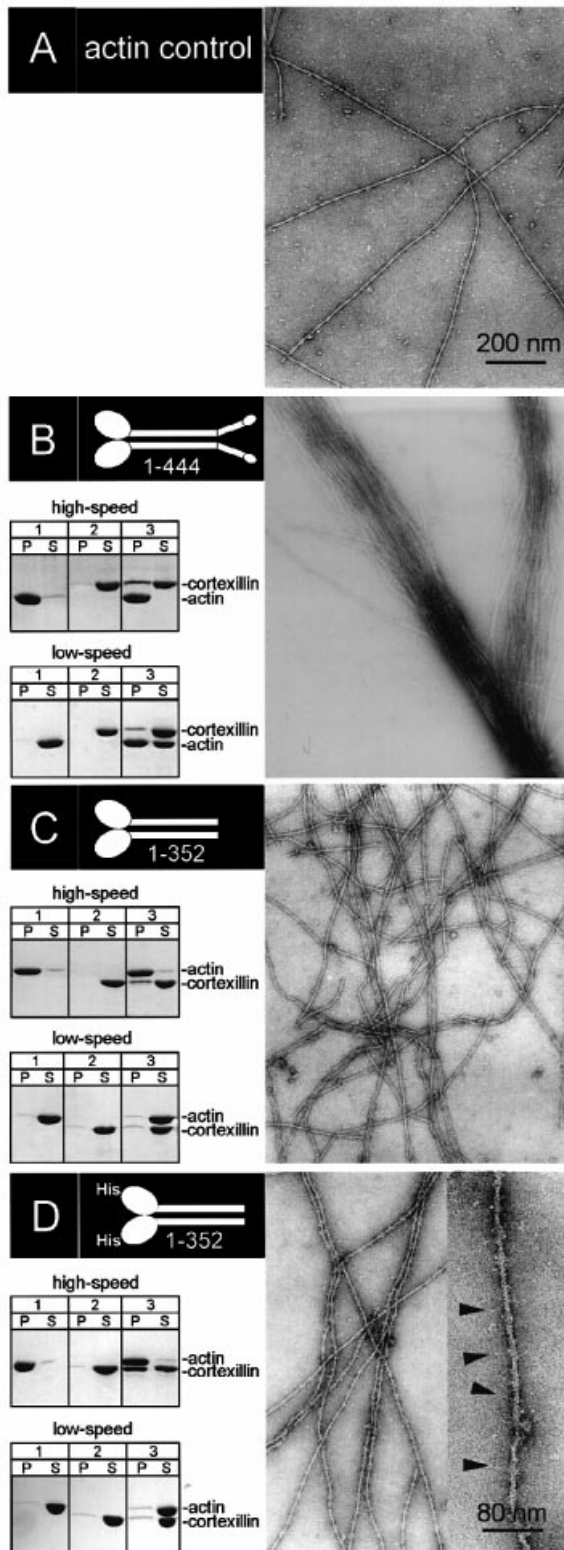

Fig. 1. Activity of the N-terminal actin-binding domain. Electron micrographs show negatively stained preparations of control actin filaments stabilized by phalloidin (**A**), of bundles formed by incubating actin with full-length cortexillin I (**B**), of loosely associated filaments formed with C-terminally truncated cortexillin I either without (**C**) or with a His-tag at the N-terminus of each subunit (**D**). In the inset of (D), the coiled-coil rods of the tailless cortexillin I molecules sticking out of the actin filaments are indicated by arrowheads. The Coomassie Blue-stained SDS–polyacrylamide gels on the left show the fractionation of actin and cortexillin I constructs into pellet (P) and supernatant (S) after high- and low-speed centrifugation. Pairs of lanes show free polymerized actin (1), free cortexillin I constructs (2), and complexes of polymerized actin with cortexillin I constructs (3). High-speed centrifugation revealed that all cortexillin I constructs did bind to filamentous actin, most vigorously the His-tagged one. Low-speed centrifugation indicated that only the full-length cortexillin I efficiently cross-linked actin filaments to form pelletable complexes. Monomer concentrations were 5 µM for actin and 5 µM for each of the cortexillin I constructs.
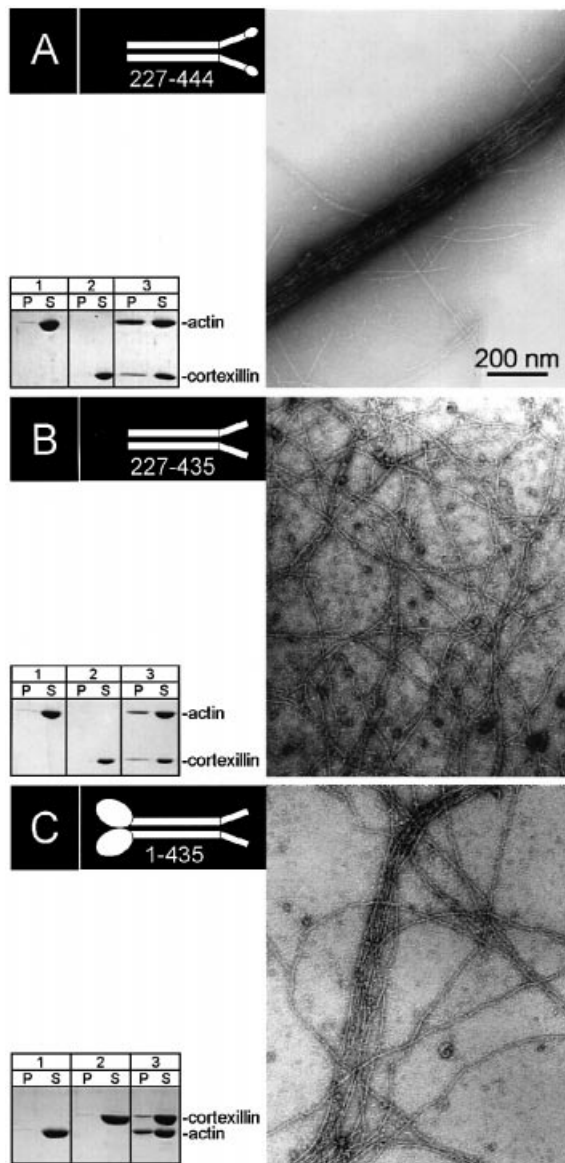
Fig. 2. Role of the C-terminal domains in the bundling of actin filaments. Actin was incubated with cortexillin I constructs as in Figure 1. The electron micrographs are paralleled by gels showing fractionation of actin filaments and cortexillin constructs by low-speed centrifugation. (**A**) shows that headless cortexillin I can form compact bundles. (**B**) demonstrates that this activity depends on the presence of the nonapeptide sequence at the end of the tail domain. In the absence of this nonapeptide only loose bundles are observed. (**C**) reveals that the presence of N-terminal actin-binding domains cannot compensate for the lack of the C-terminal nonapeptide sequence. Monomer concentrations were 5 μM for actin and cortexillin I constructs as in Figure 1.

of this nonapeptide piece in the construct CI(227–435) strongly reduced but did not completely abolish the actin-bundling activity; loose bundles were still induced (Figure 2B). A similar result was obtained with the construct CI(1–435), indicating that the N-terminal actin-binding domains did not restore the formation of compact bundles (Figure 2C).

The headless fragments shown in Figure 2 still contained the central coiled-coil region responsible for the dimerization of cortexillin I. To assay the actin-binding activity of the C-terminal monomer, a fragment comprising residues
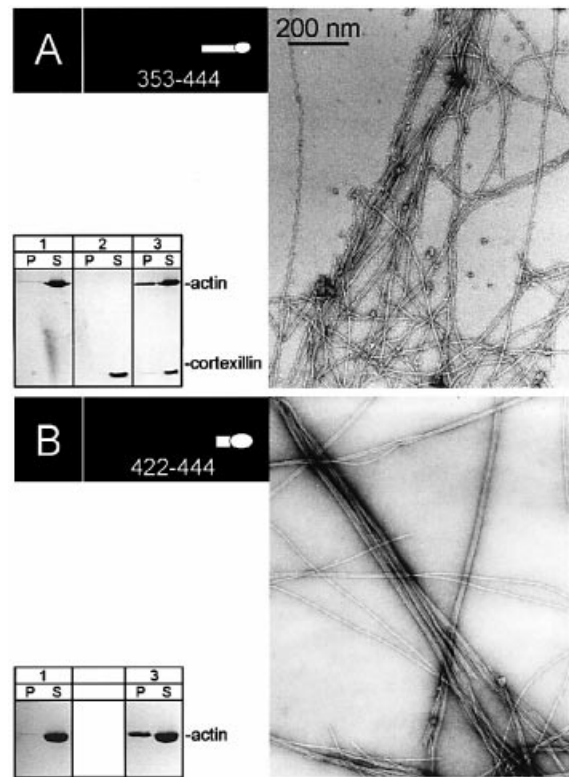

Fig. 3. Bundling activity of monomeric cortexillin I fragments lacking the dimeric coiled-coil rod region. (**A**) As revealed by electron microscopy and low-speed centrifugation, a fragment comprising the complete C-terminal domain formed loose actin bundles and caused actin filaments to pellet. (**B**) A 23mer C-terminal peptide bundled actin filaments when it was added at 5-fold molar excess over actin monomers. This 23mer peptide was too small to show up in the gel. Experiments were performed as in Figure 2, except that the concentration of the peptide in (B) was 25 μM. The monomeric state of both fragments was confirmed by analytical ultracentrifugation.

353–444 of cortexillin I was prepared. The monomeric state of CI(353–444) was confirmed by analytical ultracentrifugation under the same conditions as used in the bundling assay. Low-speed centrifugation as well as electron microscopy showed that actin filaments were bundled, indicating that the C-terminal region of each cortexillin I subunit can interact with at least two actin filaments (Figure 3A).

The contribution of the C-terminal nonapeptide sequence to actin bundling is emphasized by the activity of a synthetic peptide corresponding to residues 422–444 of the cortexillin I sequence. According to analytical ultracentrifugation, this 23mer peptide existed as a monomer. Nevertheless, it caused actin filaments to line up into compact bundles (Figure 3B). However, a 5-fold molar excess of the 23mer over actin subunits was necessary for efficient bundling. At the same molar excess, a scrambled 23mer sequence of the same amino acid residues exhibited no bundling activity (for the sequence see Materials and methods). This result indicates that not only the net charge, but also the sequence context, is important. Remarkably lysine residues are localized at every fifth position over the entire length of the C-terminal 23mer (asterisks in Figure 4A), and these positive charges might be involved in binding multiple actin filaments to the face of the peptide.
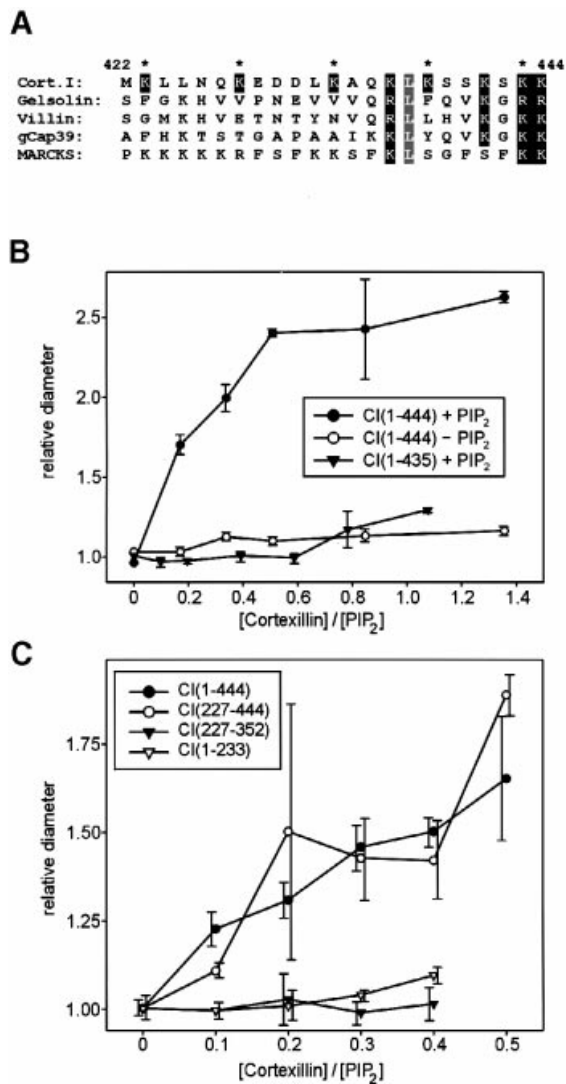
Fig. 4. Interaction of the C-terminal sequence of cortexillin I with PIP$_2$. (**A**) Sequence relationship of the C-terminal end of cortexillin I to PIP$_2$-binding motifs in human gelsolin (147–169), human villin (122–144), the 39 kDa human actin-capping protein (124–146), and human MARCKS (151–173). The asterisks point to lysine residues in the cortexillin I sequence at every fifth position. (B and C) Interaction of cortexillin I constructs with PIP$_2$-containing vesicles as determined by a dynamic light-scattering assay. (**B**) Full-length cortexillin I [CI(1–444)] interacted strongly with PIP$_2$-containing vesicles, but not with vesicles lacking PIP$_2$. The truncated construct CI(1–435), in which the PIP$_2$-binding motif was deleted, did not interact significantly with the PIP$_2$-containing vesicles. (**C**) A fragment lacking the N-terminal actin-binding domain [CI(227–444)] interacted with PIP$_2$-containing vesicles similarly to full-length cortexillin I [CI(1–444)]. Neither the rod domain [CI(227–352)] nor the N-terminal actin-binding domain [CI(1–233)] alone interacted with these vesicles. For (B) the vesicles were composed of phosphatidylcholine, phosphatidylserine and phosphatidylethanolamine (50:20:30) with or without the addition of 10% PIP$_2$ in place of 10% PC. For (C) the vesicles contained PC with 10% PIP$_2$. Numbers on the abscissa are molar ratios of cortexillin I constructs over PIP$_2$ (or corresponding amounts of PIP$_2$-free vesicles). Bars represent estimates of standard deviations.

The C-terminal end of cortexillin I binds PIP$_2$

The sequence of the C-terminal nonapeptide of cortexillin I matches a pattern known to specify PIP$_2$-binding motifs in various other actin-binding proteins (Figure 4A). The consensus motif comprises basic residues in positions 1,

6, 8 and 9, and a leucine residue in position 2. For comparison, MARCKS lacks the basic residue in position 6, but it contains lysine clusters upstream of the nonapeptide. Despite these positively charged clusters, MARCKS shows much weaker binding to PIP$_2$ than gelsolin or villin (Janmey *et al.*, 1992). The nonapeptide of cortexillin I is distinguished from the other sequences by an additional lysine residue in position 3 and three serine residues separating the positive charges.

Using a dynamic light-scattering assay for vesicle aggregation as a measure of protein binding to lipid vesicles, cortexillin I proved to interact strongly with PIP$_2$-containing vesicles (Figure 4B). It did not detectably bind to vesicles comprised of phosphatidylcholine, phosphatidylethanolamine, and phosphatidylserine. The C-terminal nonapeptide sequence proved to be crucial for the interaction with PIP$_2$-containing vesicles. After elimination of this consensus motif only insignificant PIP$_2$-binding activity of the protein was retained (Figure 4B).

The importance of the C-terminal nonapeptide for the interaction of cortexillin I with PIP$_2$ was further emphasized by the headless CI(227–444) construct, used in comparison with fragments CI(1–233) and CI(227–352), which represent either the N-terminal actin-binding domain or the coiled-coil region. Only the headless construct containing the C-terminal nonapeptide interacted with PIP$_2$ similar to full-length cortexillin I (Figure 4C).

PIP$_2$ inhibits the actin-bundling activity of cortexillin I

The importance of the C-terminal nonapeptide of cortexillin I for both the binding to PIP$_2$ and the bundling of actin filaments prompted us to test whether complexes of cortexillin I with PIP$_2$ are still capable of bundling actin filaments. Full-length cortexillin I and two N-terminally truncated constructs were incubated with actin in the presence of a 10-fold molar excess of PIP$_2$ over PIP$_2$-binding sites in cortexillin I. Since divalent cations cause PIP$_2$ micelles to aggregate (Flanagan *et al.*, 1997), actin was depleted of divalent cations for these assays. A buffer supplemented with EGTA was used (Valentin-Ranc and Carlier, 1991) and actin polymerization initiated by 50 mM KCl.

All three constructs tested, full-length cortexillin I, the headless construct CI(227–444) and the peptide CI(422–444), bundled actin filaments in the absence of divalent cations, as they did under the standard conditions used previously (Figure 5, left panels; compare with Figures 1B, 2A and 3B). In all three cases the bundling activity was strongly attenuated by the addition of PIP$_2$ micelles (Figure 5, right panels).

Actin filaments appeared to be bent by complexes of PIP$_2$ and cortexillin I or its C-terminal fragments. At a high magnification, numerous globular structures with diameters of 10–20 nm were associated with the actin filaments (Figure 5B–D). There was also considerable background of unbound PIP$_2$–cortexillin I micelles on the carbon-coated support of the electron microscope grids. In the absence of cortexillin I, PIP$_2$ did not bend the actin filaments, and globular structures, probably PIP$_2$ micelles, were rarely seen (Figure 5A). Taken together, these data suggest that PIP$_2$–cortexillin I complexes interact with actin filaments, irrespective of their low bundling activity.
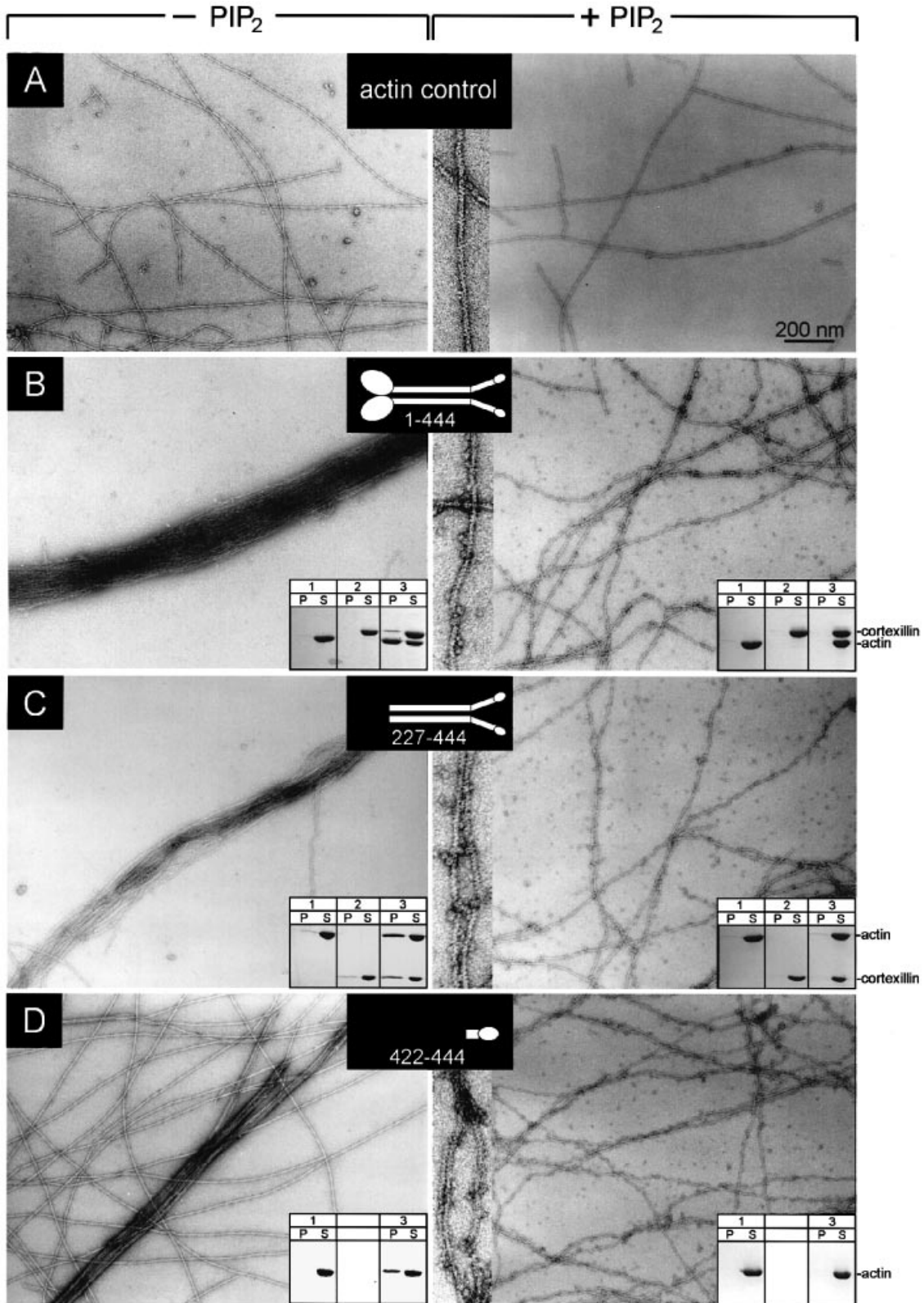
Fig. 5. Inhibition of the actin-bundling activity of cortexillin I constructs by PIP$_2$. EGTA-treated actin was incubated without (**A**) or with (**B**–**D**) cortexillin I constructs in divalent cation-free polymerization buffer. The left panels depict controls without PIP$_2$ to demonstrate that the actin-bundling activity shown in Figures 1–3 was not affected by the absence of divalent cations. The right panels show corresponding preparations to which micelles of PIP$_2$ were added. Images show electron micrographs of negatively stained specimens. In the right panels, details are illustrated at 3.5-fold higher magnification than in the main images. Insets show pellet (P) and supernatant (S) fractions after low-speed centrifugation. Concentrations of actin and cortexillin I constructs were the same as in Figures 1–3. Again, a 5-fold molar excess of the peptide CI(422–444) over actin was added in (D).

Activities of C-terminal cortexillin I constructs in vivo

The activities of cortexillin I fragments *in vitro* established a predominant role of the C-terminal region in the binding of PIP_2 and the bundling of actin filaments. Data obtained *in vivo* documented that a C-terminal fragment tagged with GFP was translocated to the cleavage furrow and was capable of rescuing cytokinesis in cortexillin I-null cells (Weber *et al.*, 1999). To evaluate the role of the basic nonapeptide at the C-terminal end of this fragment in cytokinesis, we investigated fragment CI(352–435) lacking the nonapeptide and the oligopeptide CI(436–444) comprising the nonapeptide sequence in comparison with CI(352–444), the fragment representing the entire C-terminal domain. All three fragments were fused at their N-terminus to GFP, and the fusions were used to complement cortexillin I-null cells (Figure 6).

The C-terminally truncated CI(352–435) fragment and CI(352–444) were expressed to about the same degree, the C-terminal nonapeptide CI(436–444) in a 4-fold excess (Figure 6A).

As reported previously (Faix *et al.*, 1996; Weber *et al.*, 1999), the cortexillin I-null mutant produced many multinucleate cells in suspension cultures, and this deficiency in cytokinesis was compensated by expression of the complete C-terminal domain, i.e. the fragment CI(352–444) (Figure 6B and C). An intermediate pattern of mono- and multinucleate cells was observed in the same mutant complemented with CI(352–435), indicating that a basal activity in cytokinesis was retained in the absence of the C-terminal PIP_2-binding nonapeptide. No such activity was found in the mutant cells producing CI(436–444). Numerous multinucleate cells showed that the GFP-fusion of this nonapeptide alone did not rescue cytokinesis.

Rescue of cytokinesis may depend (i) on the distribution of a cortexillin I fragment between the cytoplasm and the cell cortex; (ii) on the efficiency of its translocation to the mid-zone of a cell during mitosis; and (iii) on its potential to provide the furrow region with the mechanical properties required for cleavage. In an attempt to distinguish between these possibilities, GFP fluorescence of the three C-terminal cortexillin I constructs was recorded to monitor their redistribution in dividing cells (Figure 7). The complete C-terminal domain, i.e. CI(352–444), was

used as a reference because of its strong accumulation in the cell cortex and its efficient translocation to the mid-zone at the onset of cytokinesis (Figure 7A). When the C-terminal nonapeptide was eliminated, more label resided in the cytoplasm. Nevertheless, the CI(352–435) fragment was clearly enriched in the cortex of the cleavage furrow relative to the poles of a dividing cell (Figure 7B and C). The GFP-fusion of the C-terminal
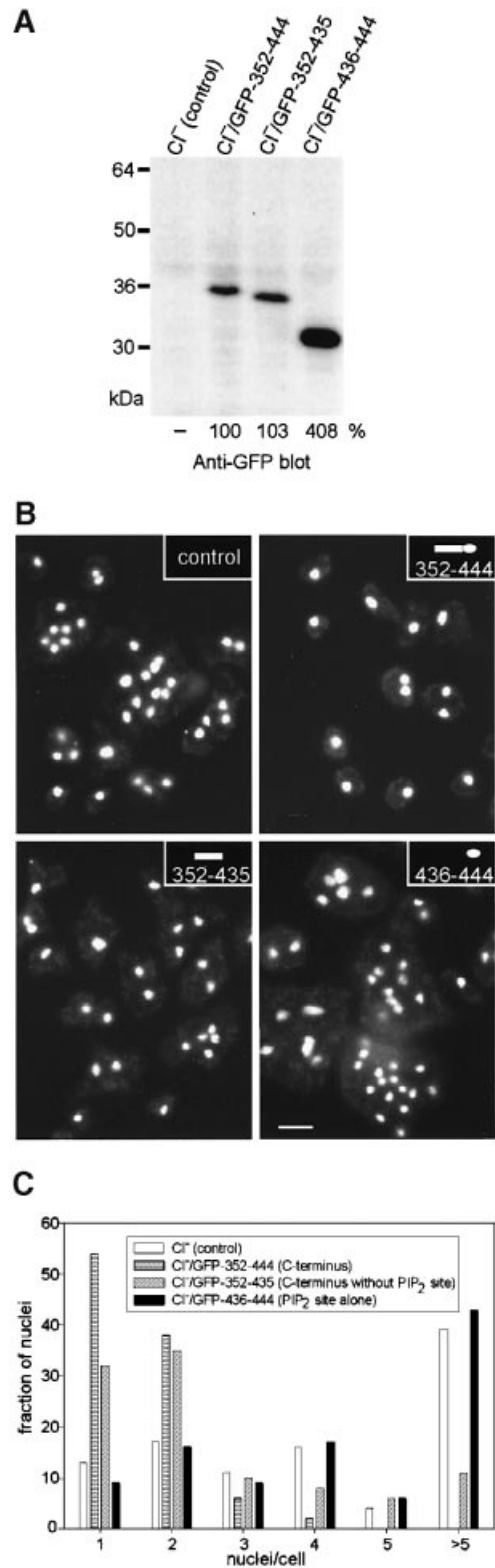

Fig. 6. Rescue of cytokinesis by C-terminal cortexillin I fragments tagged with GFP. (**A**) Blot of total cellular proteins in a cortexillin I-null mutant (CI⁻, control) and in the same mutant transformed with GFP-fusions of the complete C-terminal domain CI(352–444), of the C-terminal domain without the PIP_2-binding site CI(352–435), or of the PIP_2-binding motif alone CI(436–444). (In comparison to the C-terminal fragment used *in vitro*, one additional residue, Arg352, was left between GFP and cortexillin I portions.) The blot was indirectly labeled with [¹²⁵I]anti-GFP mAb, and percentages of bound antibody relative to the complete C-terminal domain are indicated below the lanes. (**B**) In cells of the same strains as in (A), cultivated with nutrient medium in shaken suspension, the nuclei were stained with DAPI to illustrate the relation of mono- to multinucleate cells. Bar, 10 μm. (**C**) Histogram showing the distribution of the number of nuclei in control CI-null cells and in CI-null cells complemented with the three GFP-tagged C-terminal fragments analyzed. A total of 500–750 nuclei were counted for each strain. These data show the rescue of cytokinesis by the complete C-terminal region and establish a partial rescue by the truncated fragment missing the PIP_2-binding site. The GFP-tagged PIP_2-binding motif alone was inefficient in rescuing cytokinesis.
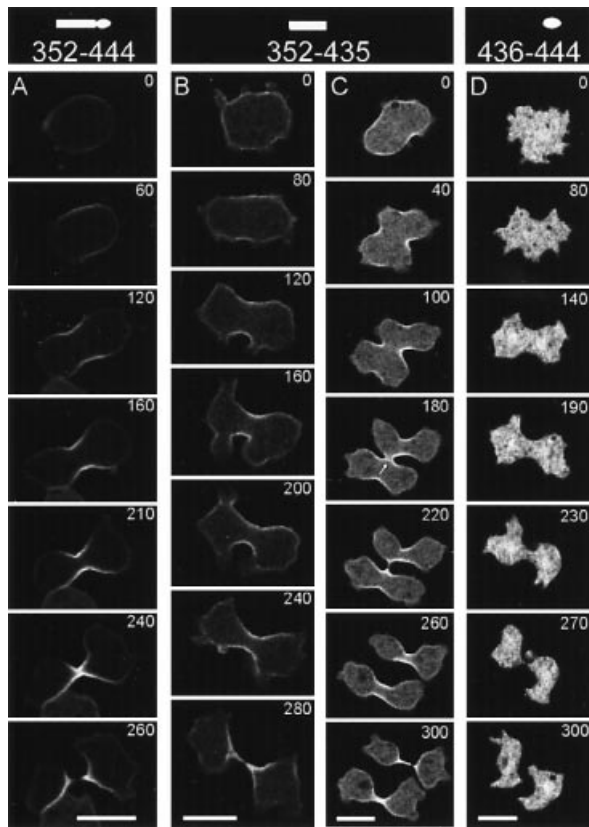
Fig. 7. Mitotic re-localization of three C-terminal cortexillin I fragments (top panels). As in Figure 6, the constructs were tagged at their N-terminus with GFP and expressed in cortexillin I-null cells. Confocal fluorescence images were taken at the times indicated in seconds. (**A**) The complete C-terminal domain showed prominent cortical localization. Accumulation in the cleavage furrow started shortly before the formation of a cleavage furrow. (B and C) The C-terminally truncated domain, GFP-CI(352–435), was less stringently enriched in the cell cortex but was re-localized to the furrow region. In (**B**), accumulation of the GFP-fusion protein started at the same stage as in (A), shortly before the furrow ingressed. The cell in (**C**) was binucleate and therefore produced four daughter cells. The sequence shows how the cortexillin I accumulated in the central region participated in the formation of the first furrow and subsequently of the second one (180 s and following frames). This example illustrates the tight coupling between cortexillin I redistribution and progression of the cleavage furrow. (**D**) The C-terminal nonapeptide, GFP-CI(436–444), was distributed within the cytoplasm and slightly enriched in the nucleus. Bars, 10 μm.

Table I. GFP constructs in the cortex and cytoplasm

Ratio of fluorescence intensities (R^a)	352-444	352-435
R_{furrow}	6.1 ± 1.1	3.4 ± 0.7
R_{poles}	3.0 ± 0.6	1.8 ± 0.2
R_{furrow} / R_{poles}	2.1 ± 0.5	1.9 ± 0.2

Values are means $\pm$ SD from seven cells.
[a]Fluorescence intensity in the cortex divided by intensity in the cytoplasm.

Discussion

Different modules in the cortexillin I molecule act together in the assembly of actin filaments

An overview of cortexillin I constructs and their inter-actions with actin and PIP$_2$ is given in Table II. Functional domains are located in the N- and C-terminal regions of each subunit, and are separated by a parallel two-stranded coiled-coil rod consisting of exactly 18 heptad repeats (Faix *et al.*, 1996; Steinmetz *et al.*, 1998). Based on the crystal structure of this rod, an atomic model indicates that both the N- and C-terminal end segments of the rod region, i.e. residues 227–242 and residues 344–352, are disordered (Burkhard *et al.*, 1998). The flexibility of these segments may allow the N- and C-terminal domains of cortexillin I to bend and swivel so as to interact with actin filaments optimally.

In accordance with the sequence homology of the N-terminal domain to actin-binding sites of the α-actinin/spectrin type (Faix *et al.*, 1996), a dimer containing two of these domains binds to actin (Figure 1C and D). However, this tailless cortexillin I dimer has only a low bundling activity, indicating that the two N-terminal 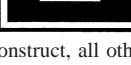domains of the molecule tend to bind to the same actin filament rather than to two separate filaments. In contrast, headless cortexillin I causes actin filaments to form compact bundles (Figure 2A). Even a monomeric C-terminal fragment is capable of inducing loose bundles, indicating that each of the C-terminal domains of cortexillin I can interact with at least two actin filaments (Figure 3A).

The basic stretch of nine amino acid residues at the C-terminal end of the cortexillin I sequence has a strong impact on actin filament bundling, and this stretch is essential for PIP$_2$ binding (Figure 4). Whereas PIP$_2$ leaves the N-terminal domains unaffected, it strongly attenuates the bundling activity of the C-terminal domains of cortexillin I (Figure 5). This finding establishes that actin-bundling and PIP$_2$-binding activities overlap at the C-terminal end of cortexillin I. Taken together these data suggest that one cortexillin I homodimer can bind to at least five actin filaments.

Extrapolating the data obtained *in vitro* to the situation *in vivo*, the possibility has to be considered that cortexillin I forms heterodimers with cortexillin II. In the sequence of cortexillin II an N-terminal actin-binding domain of the

nonapeptide alone showed no obvious accumulation in the cell cortex (Figure 7D). This construct remained dispersed throughout the cytoplasm, with a slight enrichment in the nucleus.

To compare the localization of CI(352–435) and CI(352–444) during cell division in quantitative terms, fluorescence intensities of the GFP-fusion proteins were determined along transverse lines through the cleavage furrow and polar regions. The data shown in Table I confirm that removal of the C-terminal nonapeptide attenu-ated association with the cell cortex. Remarkably, when the amount of protein accumulated in the cortex of the furrow region and of the poles was compared, the ratio turned out to be almost the same in the presence and absence of the nonapeptide sequence.

Table II. Cortexillin I constructs and their activities *in vitro*

Construct	Symbol	Mass of Monomer	Isoelectric Point	Actin Bundling		PIP$_2$-binding
CI (1-444)		50.5 kDa	6.2	53 %	(Figure 1B)	yes
CI (1-435)		49.5 kDa	5.4	24 %	(Figure 2C)	no
CI (1-352)		40.3 kDa	5.5	1 %	(Figure 1D)	not determined
CI (1-233)		26.6 kDa	5.6	0 %	(not shown)	no
CI (227-444)		24.7 kDa	6.9	37 %	(Figure 2A)	yes
CI (227-435)		23.7 kDa	5.3	16 %	(Figure 2B)	not determined
CI (353-444)		10.2 kDa	9.1	15 %	(Figure 3A)	not determined
CI (422-444)		2.7 kDa	10.8	29 % (5-fold excess)	(Figure 3B)	yes
CI (227-352)		14.6 kDa	5.4	not determined		no

CI(1–444) is the full-length construct, all other constructs are C-terminally or N-terminally truncated. CI(422–444) is a synthetic peptide. Isoelectric points have been calculated by the UWGCG program 'isoelectric'. Bundling of actin filaments was quantified by scanning the actin bands in Coomassie Blue-stained gels after low-speed centrifugation. Percentages are pelleted over total actin. The figures in parentheses provide evidence by electron microscopy for the bundling of actin filaments. PIP$_2$ binding was determined using the light-scattering assay (Figure 4B and C) except for CI(422–444), whose PIP$_2$ binding was inferred from the inhibition of actin bundling. In all constructs that bound PIP$_2$, the actin-bundling activity was inhibited by micellar PIP$_2$.

α-actinin/spectrin type is readily identified; however, no C-terminal PIP$_2$ binding motif is recognizable (Faix *et al.*, 1996). In order to study *in vivo* the function of the C-terminal domain of cortexillin I independent of any dimer formation, we have expressed C-terminal fragments lacking the coiled-coil rod sequence. These monomeric fragments were tagged with GFP at their N-terminus and used to complement cortexillin I-null mutants.

Sequence requirements for C-terminal domain activities in vivo

The involvement of cortexillins in cytokinesis can be subdivided into two functions: first, to couple to the machinery which translocates cortical proteins to the cleavage furrow; and second, to provide the furrow with the mechanical properties required for cleaving the cell. Both activities reside in the C-terminal cortexillin I segment consisting of residues Arg352 to Lys444. The question was whether the nonapeptide motif of residues 436–444 is essential for the function of cortexillin I *in vivo*, or whether this motif only reinforces activities that reside in other sequence elements of the C-terminal cortexillin I segment. Our results demonstrate that the nonapeptide motif enhances the affinity of cortexillin I for targets that reside in the cell cortex (Figure 7 and Table I) and accordingly improves the rescue of cytokinesis in cortexillin I-null mutants (Figure 6).

Although these findings establish a function *in vivo* of the nonapeptide motif at the C-terminal end of cortexillin I, they likewise attribute a salient activity to the region flanked by Arg352 and Gln435 in the capacity of cortexillin I to support cytokinesis. The GFP-tagged CI(352–435) fragment lacking the nonapeptide motif still accumulates in the cleavage furrow, where it exerts a residual activity of rescuing cytokinesis (Figure 6B and C, and Figure 7B and C). A pertinent question concerning this region is how it is targeted to the cell cortex. *In vitro*, cortexillin I lacking the nonapeptide still causes association of actin filaments into loose bundles (Figure 2B), and it may also bind to lipids other than PIP$_2$ (P.Janmey, unpublished results). Characteristically, cortexillin I and its C-terminal fragments accumulate specifically at the cell periphery but not at the membranes of various organelles (Figure 7). This specificity in localization contrasts with that of vacuolins A and B that associate with late endosomes (Rauchenberger *et al.*, 1997) or of drainin that binds to the outer surface of the contractile vacuole (Becker *et al.*, 1999). None of these proteins aligns beneath the plasma membrane as observed for cortexillin I. Further work on structure–function relationships will concentrate on the 84-residue stretch between Arg352 and Gln435 of the cortexillin I sequence.

Cortexillin I translocation and mitotic cortical flow

Based on the translocation of the C-terminal cortexillin I fragment CI(352–435), which binds to actin but no longer to PIP$_2$, we suggest a myosin II-independent actin flow in the cortex of mitotic cells that carries proteins from the cell poles towards the cleavage furrow. In myosin II-null cells a transport system has been demonstrated to which

membrane proteins can be coupled. Proteins that are cross-linked on the cell surface with concanavalin A at the onset of cytokinesis are rapidly depleted from a circumscribed area around the microtubule asters, and are accumulated in the mid-zone where the furrow is formed (Weber *et al.*, 1999). Cortexillin I is redistributed on the inside of the plasma membrane in a pattern similar to the concanavalin A-linked proteins on the outside.

We assume that cortexillin I is directly bound, and cross-linked membrane proteins are indirectly coupled, to actin filaments that are translocated from the poles to the mid-zone of a dividing cell. The direction of this flow towards the incipient cleavage furrow appears to depend on the microtubule asters, since in *Dictyostelium* the spindle is not required for the formation of a cleavage furrow (Neujahr *et al.*, 1998 and Figure 7C of this paper). Candidate motors for driving the translocation of actin are any of the unconventional myosins in *Dictyostelium* cells whose functions have not yet been identified (Titus, 1997). The conventional myosin II is not only dispensable for mitotic cortical flow; even its association with actin filaments during transport to the cleavage furrow has been questioned (Zang and Spudich, 1998).

Net transport of actin filaments to the mid-zone should result in a ring of accumulated actin in the cleavage furrow. However, labeling of fixed cells with tetramethyl-rhodamine isothiocyanate-phalloidin or recording of GFP–actin in living cells has provided evidence against a substantial accumulation of filamentous or total actin in the furrow region of *Dictyostelium* cells (Neujahr *et al.*, 1997a,b). Therefore, mid-zone depolymerization is crucial for the proposed actin cycling in mitotic cells to work. Unpublished data indicate that an actin flow exists in mitotic *Dictyostelium* cells, and work is in progress to provide evidence for the proposed mid-zone depolymerization.

Materials and methods

Purification of recombinant cortexillin I fragments from E.coli
Cortexillin I cDNA was used as a template for PCR of DNA encoding the entire coding region of cortexillin I [denoted CI(1–444)] or fragments thereof. For cloning into the pQE-32 His-tag vector the primers were designed to introduce a *Bam*HI site at the 5′ end and a *Hin*dIII site at the 3′ end, as well as a factor Xa cleavage site. For cloning CI(1–444) into the ATG-vector pQE-60, a *Nco*I site was used at the 5′ end and a *Bam*HI site at the 3′ end. The 3′-terminal construct encoding amino acids 353–444 [CI(353–444)] was cloned into a GST-fusion vector using a *Bam*HI site at the 5′ end and a *Sal*I site at the 3′ end. The amplified products were cloned into the expression vectors pQE-32, pQE-60 (Qiagen) or pGEX-5X-1 (Pharmacia and Upjohn, Uppsala, Sweden). All coding sequences were verified. The constructs were expressed in *E.coli* M15 (Qiagen).

Unmodified full-length cortexillin I encoded by the ATG construct of CI(1–444) was purified by anion-exchange chromatography on a DE-52 and a MonoQ column. His-tagged or GST-fusion proteins were purified from the soluble fraction of bacterial extracts using Ni^{2+}–NTA–agarose affinity columns (Qiagen) or glutathione–Sepharose affinity columns (Pharmacia). The His-tag or GST-fusion proteins which contained the factor Xa site IEGR were cleaved and purified essentially as described by Humm *et al.* (1997).

Electron microscopy
Actin was purified from rabbit skeletal muscle as described by Rees and Young (1967). F-actin bundles were obtained from mixtures of G-actin with cortexillin I constructs in polymerization buffer, pH 7.0 (10 mM MOPS, 2 mM $MgCl_2$, 50 mM KCl, 0.5 mM 2-mercaptoethanol) and stoichiometric amounts of phalloidin relative to actin within 2 h (Bremer *et al.*, 1994). Samples were adsorbed for 30 s to a glow-discharged carbon-coated collodion film on a copper grid (Aebi and Pollard, 1987). The grid was then washed on two drops of distilled water before it was sequentially stained on two drops of 0.75% uranyl formate pH 4.25, for a total of 15 s. Electron micrographs were taken in a Hitachi H-7000 TEM operated at 100 kV on Kodak SO-163 electron image film at ×50 000 and ×30 000 nominal magnification as calibrated according to Wrigley (1968).

F-actin co-sedimentation assays
G-actin was purified from rabbit skeletal muscle as for electron micrographs. For high-speed co-sedimentation assays, solutions of G-actin and cortexillin I constructs were cleared for 30 min in the cold at 100 000 *g* in a Beckman table top ultracentrifuge TL-100, before the samples were mixed and incubated for 2 h at room temperature in Beckman centrifugation tubes in polymerization buffer (pH 7.0). Subsequently, the reaction mixtures were centrifuged as above for 1 h in the ultracentrifuge, and the pellets and supernatants loaded separately on SDS–polyacrylamide gels.

For low-speed co-sedimentation, the proteins were cleared as above and then incubated for 2 h in polymerization buffer pH 7.0. Subsequently, the samples were pelleted in the cold for 1 h at 15 000 *g* in an Eppendorf centrifuge, and analyzed by SDS–PAGE in the supernatant and pellet fractions.

For quantitative analysis of the low-speed co-sedimentation assays (Table II) the Coomassie Blue-stained gels were scanned. From the digitized data the percentages of pelleted actin were calculated using the Optimas image-processing program (Optimas Corporation, Bothell, WA).

Inhibition of actin bundling by PIP2
Divalent cation-free actin was prepared immediately before use by incubating Ca^{2+}–ATP–G-actin with 1 mM EGTA for 10 min on ice (Valentin-Ranc and Carlier, 1991). The divalent cation-free actin was polymerized together with cortexillin I constructs in polymerization buffer pH 7.0, lacking $MgCl_2$.

PIP_2 was hydrated in 10 mM Tris-buffer pH 7.0 to 0.5 mg/ml and sonicated as described by Janmey and Stossel (1989). The PIP_2 micelles were added to the mixture of cortexillin I (fragments) and actin in a 10-fold molar excess over actin. After incubation for 2 h, the samples were prepared for electron microscopy or used for co-sedimentation assays.

Preparation of phospholipid vesicles
Phospholipid vesicles were prepared by adding phosphatidylcholine (PC), phosphatidylserine (PS) and phosphatidylethanolamine (PE) at a ratio of 50:20:30 from solutions of 10 mg/ml in chloroform to deliver 2 mg of total lipid into 10 ml round-bottomed glass flasks. All phospholipids were natural products obtained from Sigma Chemical (St Louis, MO). The chloroform was evaporated with a stream of dry N_2 to form a thin, even film at the bottom of the flask. The flasks were then placed in a vacuum for 30 min to dry the lipid film further.

To form control vesicles not containing PIP_2, the dried lipid films were hydrated with 1.8 ml of sucrose buffer (5 mM HEPES pH 7.4, 0.1 mM EDTA and 211 mM sucrose), 160 µl H_2O, and 40 µl 10 mM Tris buffer pH 7.0. For the preparation of PIP_2-containing vesicles, 40 µl of H_2O were replaced by 40 µl of 5 mg/ml of PIP_2 micelles in 10 mM Tris buffer pH 7.4 and a corresponding amount of PC was omitted from the dried lipid film. Under these conditions the PIP_2 transfers from micelles to the PC film to form mixed lipid bilayers (Janmey *et al.*, 1987; Janmey and Stossel, 1989). The flasks were sealed with parafilm and allowed to hydrate overnight in a 37°C water bath. Subsequently, the flasks were vortexed for a few seconds. A lipid extruder (Liposofast, Avestin, Ottawa, Ont., Canada) with a membrane pore size of 100 nm was used to form unilammellar vesicles from 500 µl of the hydrated lipid solution. The preparation was passed through the membrane 20 times, diluted in a 3 ml Beckman polycarbonate centrifuge tube 5-fold with HKE (5 mM HEPES pH 7.4, 0.1 mM EDTA and 120 mM KCl), and incubated for 1 h at room temperature. Vesicles were pelleted at 100 000 *g* for 1 h at 25°C and resuspended in 500 µl of HKE. In some cases vesicles containing only PC and PIP_2 (90:10) were formed by the method detailed in Janmey *et al.* (1987) except for the additional step of passage through the Liposofast filter. In parallel studies of binding to cortexillin constructs, no significant differences were found using the two types of mixed lipid vesicles.

Dynamic light scattering of lipid vesicles
Dynamic light scattering was performed using a Brookhaven Instruments (Holtsville, NY) BI30Atn system illuminated by a 10 mW He–Ne laser

as described by Hübner *et al.* (1998). The intensity autocorrelation functions of 200 µl samples containing 20 µg of lipid in cylindrical glass tubes were measured at an angle of 90° at 23°C. The hydrodynamic diameter of the lipid particles was calculated from the translational diffusion constant derived from a cumulative analysis of the autocorrelation function. The average diameter of different vesicle preparations varied from 160 to 190 nm. Consistent with previous findings, the Z-averaged diffusion constant was generally slightly larger than the nominal size expected from the pore size of the filter. For each measurement of the effects caused by a cortexillin I construct, aliquots of a stock solution (typically 10–100 µM of a particular construct) were added sequentially to the vesicle preparations, and the correlation functions were calculated from triplicate measurements of multiple replicates, starting 1 min after addition of the protein.

Analytical ultracentrifugation

Analytical ultracentrifugation was performed on an Optima XLA analytical ultracentrifuge (Beckman Instruments, Fullerton, CA) equipped with an absorption optical system, as described previously (Faix *et al.*, 1996). The concentration of cortexillin I fragments was adjusted to $OD_{276} = 0.1$, and the protein was analyzed at 20°C in polymerization buffer pH 7.0.

Localization of GFP-fusion constructs during cytokinesis

Construction of the GFP(S65T)–CI(352–444) fusion has been described by Weber *et al.* (1999). GFP(S65T) was combined with CI(352–435) in essentially the same way. For GFP–CI(436–444), the GFP(S65T) sequence was amplified by PCR in order to add in-frame a sequence encoding the linker peptide $(GGS)_2$ followed downstream by the last nine residues of cortexillin I. The sequences of all PCR-generated fragments were verified by DNA sequencing.

Dictyostelium discoideum cells were cultivated at 23°C axenically in nutrient medium as described by Claviez *et al.* (1982), either in shaken suspension at 150 r.p.m. or on polystyrene Petri dishes. Cortexillin I-null cells were transformed by electroporation, strains producing GFP-fusion proteins were selected on plates in nutrient medium containing 10 µg/ml of Blasticidin S (ICN, Corta Mesa, CA), and cloned on SM agar plates with *Klebsiella aerogenes*. For the immunoblot in Figure 6A, equal amounts of cellular proteins, corresponding to 2×10^5 cells of the CI⁻/GIP-352-444 strain, were loaded per lane, and the blots labeled with anti-GFP mAb 264-449-2, a gift of M.Maniak. Bound antibodies followed by ^{125}I-labeled sheep anti-mouse IgG were quantified on a Fuji phosphoimager. For the counting of nuclei, cells cultivated in shaken suspension were fixed with picric acid–formaldehyde according to Humbel and Biegelmann (1992) and stained with 4′,6-diamidino-2-phenylindole (DAPI).

Localization of GFP-fusion proteins during cytokinesis was performed as described previously (Weber *et al.*, 1999). Medial–sagittal planes through the cells were scanned at time intervals of 10 s. Fluorescence intensity profiles (Table I) were determined along 0.8 µm broad lines drawn perpendicular to the long axis of half-way constricted cells. Data were analyzed using the Optimas image-processing program (Optimas Corporation, Bothell, WA).

Peptide synthesis

The peptides were synthesized with the Fmoc/tBu strategy (Atherton *et al.*, 1981). The products were dissolved in 50 mM acetic acid and purified by preparative reverse-phase HPLC on a Nucleosil 250/C_{18} PPN column (Macherey & Nagel, D-52313 Düren, Germany) using water and acetonitrile as the mobile phases. The peptide corresponding to residues 422–444 of cortexillin I had the sequence MKLLNQKEDDLK-AQKLKSSKSKK. The sequence of the scrambled peptide was KLSKASKDKQLKDKEKMSLNLQK.

References

Aebi,U. and Pollard,T.D. (1987) A glow discharge unit to render electron microscope grids and other surfaces hydrophilic. *J. Electron Microsc. Tech.*, **7**, 29–33.

Atherton,E., Hubscher,W., Sheppard,R.C. and Woolley,V. (1981) Synthesis of a 21-residue fragment of human proinsulin by the polyamide solid phase method. *Hoppe-Seyler's Z. Physiol. Chem.*, **362**, 833–839.

Becker,M., Matzner,M. and Gerisch,G. (1999) Drainin required for membrane fusion of the contractile vacuole in *Dictyostelium* is the prototype of a protein family also represented in man. *EMBO J.*, **18**, 3305–3316.

Bremer,A., Henn,C., Goldie,K.N., Engel,A., Smith,P.R. and Aebi,U. (1994) Towards atomic interpretation of F-actin filament three-dimensional reconstruction. *J. Mol. Biol.*, **242**, 683–700.

Burkhard,P., Steinmetz,M.O., Schulthess,T., Landwehr,R., Aebi,U. and Kammerer,R.A. (1998) Crystallization and preliminary X-ray diffraction analysis of the 190 A long coiled-coil dimerization domain of the actin-bundling protein cortexillin I from *Dictyostelium discoideum. J. Struct. Biol.*, **122**, 293–296.

Claviez,M., Pagh,K., Maruta,H., Baltes,W., Fisher,P. and Gerisch,G. (1982) Electron microscopic mapping of monoclonal antibodies on the tail region of *Dictyostelium* myosin. *EMBO J.*, **1**, 1017–1022.

Faix,J. *et al.* (1996) Cortexillins, major determinants of cell shape and size, are actin-bundling proteins with a parallel coiled-coil tail. *Cell*, **86**, 631–642.

Flanagan,L.A., Cunningham,C.C., Chen,J., Prestwich,G.D., Kosik,K.S. and Janmey,P.A. (1997) The structure of divalent cation-induced aggregates of PIP_2 and their alteration by gelsolin and tau. *Biophys. J.*, **73**, 1440–1447.

Goldsmith,S.C., Pokala,N., Shen,W., Fedorov,A.A., Matsudaira,P. and Almo,S.C. (1997) The structure of an actin-crosslinking domain from human fimbrin. *Nature Struct. Biol.*, **4**, 708–712.

Hübner,S., Couvillon,A.D., Käs,J.A., Bankaitis,V.A., Vegners,R., Carpenter,C.L. and Janmey,P.A. (1998) Enhancement of phosphoinositide 3-kinase activity by membrane curvature and phosphoinositide-binding peptides. *Eur. J. Biochem.*, **258**, 846–853.

Humbel,B.M. and Biegelmann,E. (1992) A preparation protocol for postembedding immunoelectron microscopy of *Dictyostelium discoideum* cells with monoclonal antibodies. *Scan. Microsc.*, **6**, 817–825.

Humm,A., Fritsche,E., Mann,K., Göhl,M. and Huber,R. (1997) Recombinant expression and isolation of human L-arginine:glycine amidinotransferase and identification of its active-site cysteine residue. *Biochem. J.*, **322**, 771–776.

Janmey,P.A. and Stossel,T.P. (1989) Gelsolin-polyphosphoinositide interaction. Full expression of gelsolin-inhibiting function by polyphosphoinositides in vesicular form and inactivation by dilution, aggregation, or masking of the inositol head group. *J. Biol. Chem.*, **264**, 4825–4831.

Janmey,P.A., Iida,K., Yin,H.L. and Stossel,T.P. (1987) Polyphospho-inositide micelles and polyphosphoinositide containing vesicles dissociate endogenous gelsolin-actin complexes and promote actin assembly from the fast growing end of actin filaments blocked by gelsolin. *J. Biol. Chem.*, **262**, 12228–12236.

Janmey,P.A., Lamb,J., Allen,P.G. and Matsudaira,P.T. (1992) Phosphoinositide-binding peptides derived from the sequences of gelsolin and villin. *J. Biol. Chem.*, **267**, 11818–11823.

Neujahr,R., Heizer,C. and Gerisch,G. (1997a) Myosin II-independent processes in mitotic cells of *Dictyostelium discoideum*: redistribution of the nuclei, re-arrangement of the actin system and formation of the cleavage furrow. *J. Cell Sci.*, **110**, 123–137.

Neujahr,R., Heizer,C., Albrecht,R., Ecke,M., Schwartz,J.-M., Weber,I. and Gerisch G. (1997b) Three-dimensional patterns and redistribution of myosin II and actin in mitotic *Dictyostelium* cells. *J. Cell Biol.*, **139**, 1793–1804.

Neujahr,R., Albrecht,R., Köhler,J., Matzner,M., Schwartz,J.-M., Westphal,M. and Gerisch,G. (1998) Microtubule-mediated centrosome motility and the positioning of cleavage furrows in multinucleate myosin II-null cells. *J. Cell Sci.*, **111**, 1227–1240.

Rauchenberger,R., Hacker,U., Murphy,J., Niewöhner,J. and Maniak,M. (1997) Coronin and vacuolin identify consecutive stages of a late, actin-coated endocytic compartment in *Dictyostelium. Curr. Biol.*, **7**, 215–218.

Rees,M.K. and Young,M. (1967) Studies on the isolation and molecular properties of homogeneous globular actin: evidence for a single polypeptide chain. *J. Biol. Chem.*, **242**, 4449–4458.

Simson,R., Wallraff,E., Faix,J., Niewöhner,J., Gerisch,G. and Sackmann,E. (1998) Membrane bending modulus and adhesion energy of wild-type and mutant cells of *Dictyostelium* lacking talin or cortexillins. *Biophys. J.*, **74**, 514–522.

Steinmetz,M.O., Stock,A., Schulthess,T., Landwehr,R., Lustig,A., Faix,J., Gerisch,G., Aebi,U. and Kammerer,R.A. (1998) A distinct 14 residue site triggers coiled-coil formation in cortexillin I. *EMBO J.*, **17**, 1883–1891.

Titus,M.A. (1997) Unconventional myosins: new frontiers in actin-based motors. *Trends Cell Biol.*, **7**, 119–123.

Valentin-Ranc,C. and Carlier,M.F. (1991) Role of ATP-bound divalent metal ion in the conformation and function of actin. *J. Biol. Chem.*, **266**, 7668–7675.

Weber,I., Gerisch,G., Heizer,C., Murphy,J., Badelt,K., Stock,A., Schwartz,J.M. and Faix,J. (1999) Cytokinesis mediated through the recruitment of cortexillins into the cleavage furrow. *EMBO J.*, **18**, 586–594.

Wrigley,N.G. (1968) The lattice spacing of cristalline catalase as an internal standard of length in electron microscopy. *J. Ultrastruct. Res.*, **24**, 454–464.

Zang,J.-H. and Spudich,J.A. (1998) Myosin II localization during cytokinesis occurs by a mechanism that does not require its motor domain. *Proc. Natl Acad. Sci. USA*, **95**, 13652–13657.